

DTIC FILE COPY

4

GL-TR-90-0006
ENVIRONMENTAL RESEARCH PAPERS, NO. 1049

AD-A223 297

Production of NO, NO₂ and N₂O in Air
by Breakdown With High Power Microwaves:
A Preliminary Report

DONALD E. HUNTON
JOHN O. BALLENTIN
EDMUND TRZCINSKI
JOHN F. BORGHETTI
GENNARO S. FEDERICO



5 January 1990



Approved for public release; distribution unlimited.

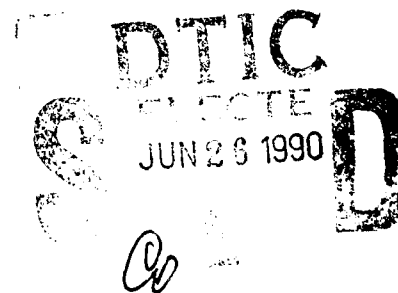


IONOSPHERIC PHYSICS DIVISION

PROJECT 2310

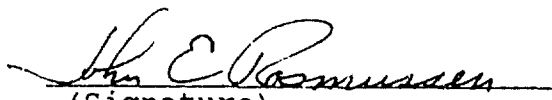
GEOPHYSICS LABORATORY

HANSCOM AFB, MA 01731-5000




90 06 25 164

"This technical report has been reviewed and is approved for publication"


(Signature)
John E. Rasmussen
Branch Chief

FOR THE COMMANDER


(Signature)
Robert A. Skrivanek
Division Director

This report has been reviewed by the ESD Public Affairs Office (PA) and is releasable to the National Technical Information Service (NTIS).

Qualified requestors may obtain additional copies from the Defense Technical Information Center. All others should apply to the National Technical Information Service.

If your address has changed, or if you wish to be removed from the mailing list, or the addressee is no longer employed by your organization, please notify GL/IMA, Hanscom AFB, MA 01731. This will assist us in maintaining a current mailing list.

Do not return copies of this report unless contractual obligations or notices on a specific document require that it be returned.

REPORT DOCUMENTATION PAGE

Form Approved
OMB No. 0704-0188

Public reporting burden for this collection of information is estimated to average 1 hour per response, including the time for reviewing instructions, searching existing data sources, gathering and maintaining the data needed, and completing and reviewing the collection of information. Send comments regarding this burden estimate or any other aspect of this collection of information, including suggestions for reducing this burden, to Washington Headquarters Services, Directorate for Information Operations and Reports, 1215 Jefferson Davis Highway, Suite 1204, Arlington, VA 22202-4302, and to the Office of Management and Budget, Paperwork Reduction Project (0704-0188), Washington, DC 20503

1. AGENCY USE ONLY (Leave blank)		2. REPORT DATE 5 January 1990		3. REPORT TYPE AND DATES COVERED Scientific, Interim	
4. TITLE AND SUBTITLE Production of NO, NO ₂ and N ₂ O in Air by Breakdown with High Power Microwaves: A Preliminary Report.				5. FUNDING NUMBERS PE 61102F PR 2310 TA G3 WU 19	
6. AUTHOR(S) Donald E. Hunton, John O. Ballenthin, Edmund Trzcinski, John F. Borghetti and Gennaro S. Federico.					
7. PERFORMING ORGANIZATION NAME(S) AND ADDRESS(ES) Geophysics Laboratory, AFSC GL/LID Hanscom AFB, MA 01731				8. PERFORMING ORGANIZATION REPORT NUMBER GL-TR-90-0006 ERP, No. 1049	
9. SPONSORING/MONITORING AGENCY NAME(S) AND ADDRESS(ES)				10. SPONSORING/MONITORING AGENCY REPORT NUMBER	
11. SUPPLEMENTARY NOTES					
12a. DISTRIBUTION/AVAILABILITY STATEMENT Approved for Public Release; distribution unlimited.				12b. DISTRIBUTION CODE	
13. ABSTRACT (Maximum 200 words) Production of trace nitrogen oxide species in air discharge plasmas was observed with a quadrupole mass spectrometer attached to a specially-designed S-band waveguide. At pressures between 25 and 200 Torr in the waveguide, nitric oxide (NO) was the most concentrated trace species observed, reaching concentrations of greater than 2% at 200 Torr. Nitrogen dioxide (NO ₂) was also observed, but only after the discharge had been turned off. NO ₂ concentrations were slightly lower than NO. At pressures between 9 and 0.3 Torr, the only species observed was nitrous oxide (N ₂ O), which reached a concentration of approximately 2% at the lower pressure. The experimental apparatus, data collection procedures, calibration procedures, data reduction, and results are described in detail.					
14. SUBJECT TERMS NO, NO ₂ , N ₂ O Microwave breakdown Mass spectroscopy, Plasma neutral chemistry (YES) ←				15. NUMBER OF PAGES 40	
				16. PRICE CODE	
17. SECURITY CLASSIFICATION OF REPORT UNCLASSIFIED	18. SECURITY CLASSIFICATION OF THIS PAGE UNCLASSIFIED	19. SECURITY CLASSIFICATION OF ABSTRACT UNCLASSIFIED	20. LIMITATION OF ABSTRACT UL		

Acknowledgements

This experiment was performed in collaboration with Ray Alvarez, Paul R. Bolton, Dave Fittinghoff and Bill Patterson of the Lawrence Livermore National Laboratory, Livermore, CA and with William T. Armstrong and Mel Buchwald of the Los Alamos National Laboratory, Los Alamos, NM. We thank the Air Force Office of Scientific Research for partial support of this experiment under Task 2310G3.

Accession For	
NTIS GRA&I	<input checked="" type="checkbox"/>
DTIC TAB	<input type="checkbox"/>
Unannounced	<input type="checkbox"/>
Justification	
By	
Distribution/	
Availability Codes	
Dist. and/or	
Dist. and/or	
A-1	



Contents

1.	INTRODUCTION	1
2.	EXPERIMENTAL APPARATUS	2
3.	EXPERIMENTAL PROCEDURES	7
4.	CALIBRATION APPARATUS	10
5.	RESULTS	11
6.	DISCUSSION	29
7.	SUMMARY	31
	REFERENCES	33

Figures

1.	Schematic Drawing of Experimental Setup	3
2.	Detail of Waveguide	5
3.	Photograph of Mass Spectrometer and Waveguide, Disassembled	8
4.	Photograph of Assembled Experiment	8
5.	Typical Incident and Reflected Pulse Shapes	9
6.	Calibration Test Stand at the Geophysics Laboratory	11
7.	Representative Mass Spectra, 200 Torr	13
8.	Representative Mass Spectra, 1 Torr	14

9.	Time History of Peak Heights, 100 Torr	15
10.	Time History of Peak Heights, 1 Torr	16
11.	Detailed Time Histories of Mass 28, 32 and Grid Current	17
12.	NO, NO ₂ and N ₂ O Calibration spectra	18
13.	NO ₂ Partial Pressure vs Time, 200 Torr	20
14.	Asymptotic NO Partial Pressures	22
15.	Asymptotic NO ₂ Partial Pressures	23
16.	Asymptotic N ₂ O Partial Pressures	23
17.	Mole Fractions of NO, NO ₂ and N ₂ O vs Waveguide Pressure	26
18.	Total Fractional Content of NO _x vs Waveguide Pressure	27
19.	Microwave Power Dependence of N ₂ O Concentration at 1 Torr	27
20.	Dependence of N ₂ O Concentration on Pulse Repetition Rate	28

Tables

1.	Peak Identifications in Air Spectra	12
2.	Summary of Experimental Conditions	21
3.	Summary of NO, NO ₂ and N ₂ O Partial Pressures	24
4.	Summary of Optical Absorption Measurements	25

Production of NO, NO₂ and N₂O in Air by Breakdown with High Power Microwaves: A Preliminary Report

1. INTRODUCTION

Breakdown in gas mixtures of N₂ and O₂, such as air, leads to formation of nitrogen oxides, NO, NO₂ and N₂O. While the appearance of these gases is well documented,^{1,2,3,4,5} the mechanisms for their formation,

(Received for Publication 2 Jan 1990)

¹Rusanov, V. D., Fridman, A. A. and Sholin, G. V. (1981) The Physics of a Chemically Active Plasma With Non-equilibrium Vibrational Excitation of Molecules, Sov. Phys.-USP. (USA), Vol. 24, No. 6, 447-74.

²Zipf, E. C. (1980) A Laboratory Study on the Formation of Nitrous Oxide by the Reaction N₂(A) + O₂ = N₂O + O, Nature, Vol. 287: 523-524.

³Park, C. (1989) A Review of Reaction Rates in High Temperature Air, AIAA-89-1740, AIAA 24th Thermophysics Conference, Buffalo, New York, June 12-14.

⁴Fraser, M. E., Tucker, T. R., Piper, L. G., and Rawlins, W. T., N₂O Production Mechanism From the Interaction of Discharge-Excited Species, Pre-publication manuscript, October, 1989.

⁵Zinn, J., Sutherland, C. D., and Roussel-Dupre, R. (1989) Chemistry Calculations Relating to AIL, Workshop on Artificial Ionized Layers in the Atmosphere, Kiev, USSR, 9-13 October.

especially of N_2O , is somewhat uncertain. In an effort to understand the chemistry leading to NO_x in air breakdown, two different techniques, mass spectroscopy and optical absorbance, were used to measure the production of trace neutral gas species in air breakdown. The optical absorbance measurement was specifically designed to measure NO_2 concentrations, whereas the mass spectrometer measured all neutral constituents.

The experiment was conducted from 6-15 September, 1989 at the Lawrence Livermore National Laboratory in Livermore, CA. Ray Alvarez, Paul Bolton, Dave Fittinghoff, and Bill Patterson of the Lawrence Livermore National Laboratory were responsible for designing and constructing the waveguide and the gas handling system. Mel Buchwald and Tom Armstrong of the Los Alamos National Laboratory conducted the optical absorbance measurements. The authors of this report from the Geophysics Laboratory were responsible for the mass spectrometer measurements. The first few days of the experiment were spent setting up and testing all of the apparatus. The data were collected on 13, 14 and 15 September.

The purpose of the present preliminary report is to document fully the experimental apparatus, measurement techniques, and the results of the mass spectrometer investigation. The optical absorption measurements will be discussed in a separate Los Alamos National Laboratory Technical Report. A complete analysis and interpretation of the data will follow in other reports.

2. EXPERIMENTAL APPARATUS

An overview of the experimental setup at the Lawrence Livermore National Laboratory is shown in Figure 1. The principal components of the apparatus are the waveguide assembly that was constructed specially for the experiment, the klystron high-power microwave source, the gas handling system *for controlling the gas environment inside the waveguide*, the components for the optical absorption measurements, and the mass spectrometer.

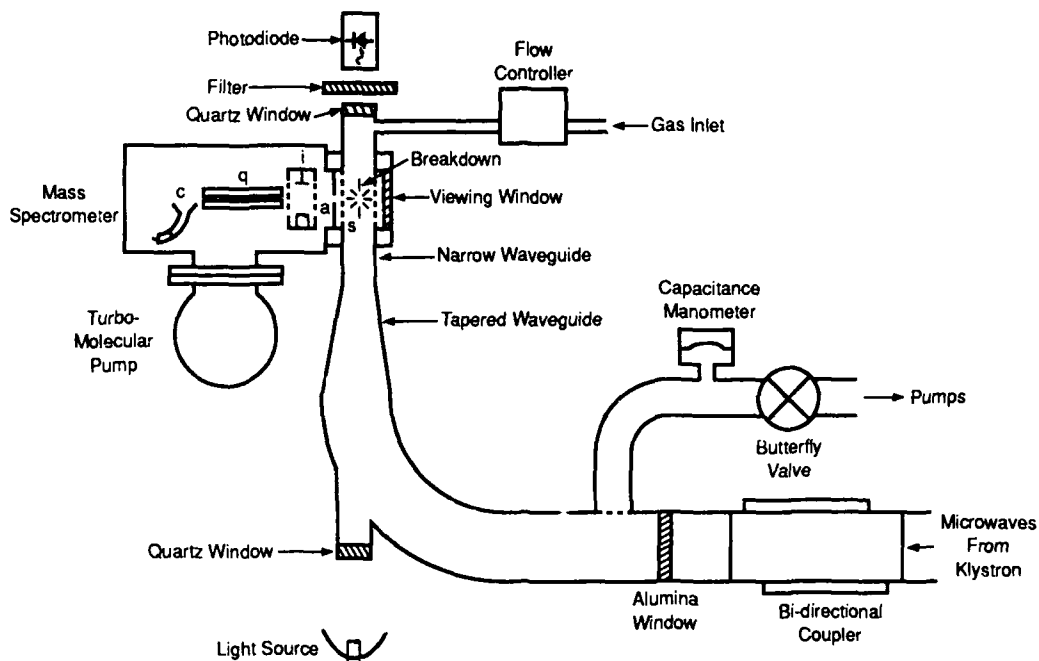


Figure 1. Schematic Drawing of Experiment Setup At Lawrence Livermore National Laboratory. The mass spectrometer parts identified by letter are: s, perforated screen in side of waveguide; a, sampling aperture; i, mass spectrometer ion source; q, quadrupole mass filter; c, Channeltron electron multiplier.

Microwaves were produced at 2.856 GHz in a high power klystron and supplied to the experiment in standard S-band WR284 waveguide sections. Microwave power was continuously adjustable from the kW range to 10 MW. The power was measured by splitting off a small fraction of the power in a bidirectional coupler and measuring its intensity with attenuators and microwave diodes. For all the experiments described here, the pulse length was 1 microsecond. The repetition rate of the pulses was continuously variable from single pulses to about 400 Hz. For the majority of the experiments here, the repetition rate was approximately 315 Hz.

The experiment waveguide section was designed to provide a long optical path length for the absorption measurements and to localize the point of the breakdown as close as possible to the mass spectrometer sampling

orifice. As shown schematically in Figure 1, a 7.5" radius, 90° curved waveguide section (with the curve in the H-plane) was attached to a 19.875" long taper, and then to a 4.8" long x 0.67 x 2.27" (inside dimensions) narrow waveguide section. The dimensions of this section were chosen to maximize the microwave field strength and therefore localize the breakdown plasma at the center of the waveguide section. In addition, two thin metal points were inserted into the waveguide through the metal screens described below to stabilize the position of the breakdown plasma. Note that in Figure 1, the plane of the narrow waveguide section has been turned 90° from its actual position for clarity in the drawing. The axis of the mass spectrometer was actually perpendicular to the plane of the drawing. The microwaves were introduced into the experiment section through an alumina window that formed a vacuum seal between the microwave source region and the experiment section.

The test gas, bottled air (AmeriGas Type UN1002) for all experiments described here, was introduced into the waveguide through an MKS 0-500 sccm automatic flow controller. The pressure in the waveguide was controlled by an MKS automatic butterfly valve in the vacuum line, while the pressure was measured with several MKS capacitance manometers. The turbopump operating through the butterfly valve had an effective pumping speed of 0 - 25 l/s. The baseline pressure in the waveguide was approximately 2×10^{-3} torr. The slowest flow that could be accurately controlled through the waveguide was 0.020 sccm. The pressure could be accurately adjusted to any value between the baseline pressure and atmospheric pressure.

The volume of the waveguide experimental section was calculated by measuring the time required to fill the waveguide to one atmosphere at a constant flow rate through the flow controllers. The result was 6.08 ± 0.05 liters.

The optical absorption experiment consisted of a high intensity quartz-halogen projector lamp placed at the bottom end of the waveguide test section, an optical filter with bandpass centered at 406.5 nm and FWHM of 41.0 nm, and a photodiode detector. The ends of the optical path in the waveguide were sealed with quartz windows. The total length of the optical

path was 1.065 m. The intensity of the lamp was stabilized with a regulated power supply and monitored with a Spectra Physics Model 404 laser power meter, which measured the intensity of the light reflected off the quartz window at the bottom of the waveguide.

A cross section through the narrow test section of the waveguide is drawn in detail in Figure 2. One-inch-diameter holes were cut into opposite faces of the waveguide and covered with perforated metal screens. The perforations in the screen were 0.031" in diameter and spaced in a 60° offset pattern with a total open area of approximately 25 percent. As shown in Figure 2, these screened openings in the wave guide were closed off with

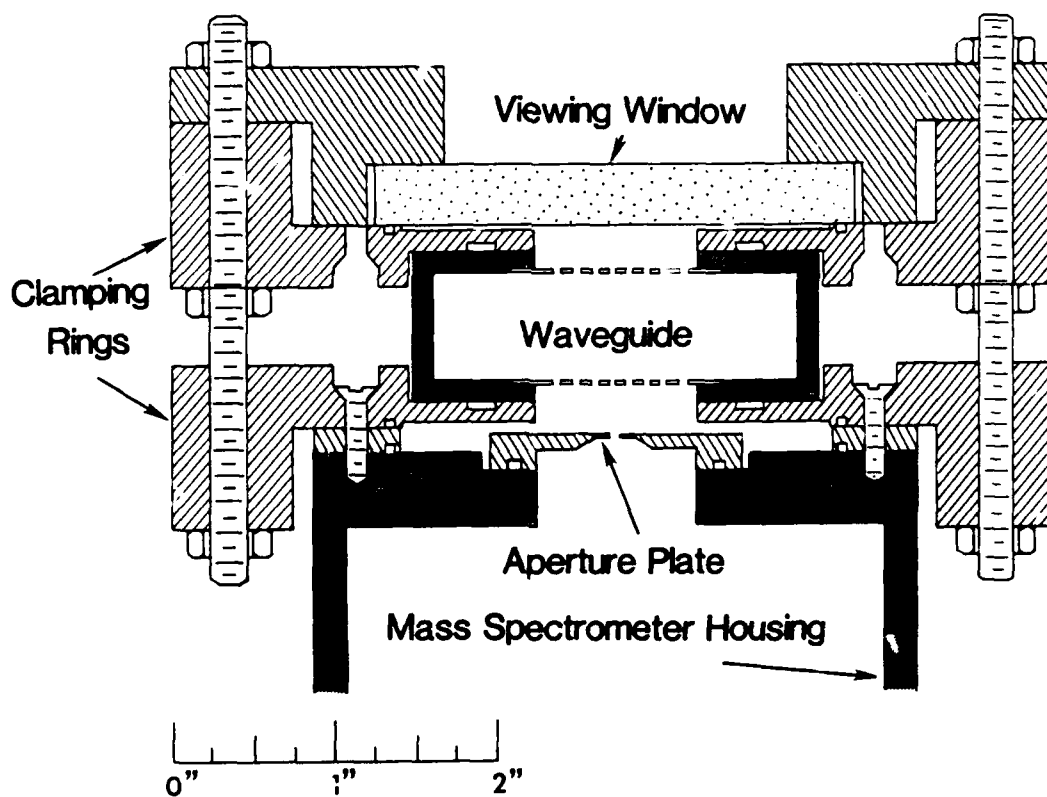


Figure 2. Detail of Waveguide. This cross-sectional drawing of the narrow test section of the waveguide shows the perforated screens in the waveguide sides, the viewing window, the mass spectrometer housing and aperture plate, and the two clamping rings that held the assembly together.

O-ring sealed clamping rings. One clamping ring held a quartz window that allowed viewing of the breakdown region, and the other clamping ring was the vacuum interface to the mass spectrometer.

The vacuum housing of the mass spectrometer was differentially pumped by a Balzers 330 l/s turbomolecular pump and was separated from the relatively high pressure waveguide by an o-ring-sealed aperture plate mounted to the front of the housing. With a 0.001" diameter aperture, the waveguide could be filled to 200 torr while maintaining an operating pressure in the mass spectrometer of approximately 7×10^{-5} torr. With a 0.005" diameter orifice, the maximum waveguide pressure was 9 torr. The background pressure in the mass spectrometer without baking was 1×10^{-7} torr.

The mass spectrometer itself was a versatile quadrupole instrument whose design was based on similar instruments flown on sounding rockets, satellites, and the Space Shuttle. Though only measurements of neutral species are reported here, the instrument was capable of detecting positive ions as well. The internal construction of the mass spectrometer was similar to instruments that have been described in previous reports⁶, so only a few significant details will be mentioned here. The ion source used a magnetically-confined transverse electron beam at an energy of 80 eV to ionize the neutral molecules that entered the mass spectrometer. The ion source was located just behind the aperture plate. A variety of grids in the ion source controlled the flux of ions. One grid, located between the electron beam and the entrance into the quadrupole mass filter, collected a constant fraction of the total ion current generated in the ion source. This current can be related to the total pressure in the ion source, and was an independent measure of the amount of signal reaching the mass filter.

The Channeltron electron multiplier was mounted behind the mass filter, and was off axis to avoid spurious counts caused by metastable neutral species or ultraviolet light. The multiplier was used in the pulse counting mode. In practice, there were no "dark" or background counts recorded, so

⁶See for example Hunton, D.E., Trzcinski, E., Wlodyka, L., Federico, G. and Dorian, J. (1986) Quadrupole Ion/Neutral Mass Spectrometer for Space Shuttle Applications, AFGL Technical Report AFGL-TR-86-0084, AF A172000, and references therein.

the baseline was at zero counts. The integration time for the pulse counter was approximately 0.01 sec. Because the Channeltron starts to saturate at about 2 MHz counting rate, the maximum number of counts per integration time was approximately 20,000. Therefore the dynamic range of the instrument was slightly greater than 10^4 .

The mass spectrometer was interfaced to a Zenith laptop computer which controlled the data taking sequences, and also displayed, reduced, and stored the data.

Figure 3 is a photograph of the mass spectrometer and the narrow waveguide test section before the clamping rings were installed. This photograph shows the aperture plate on the front of the mass spectrometer, the turbomolecular pump, the screen-covered holes in the sides of the waveguide, and, at the top of the photograph, the gas inlet and quartz window flange. Figure 4 shows the mass spectrometer fully attached to the waveguide.

3. EXPERIMENTAL PROCEDURES

The following procedure was used for most of the neutral plasma composition experiments reported here. The waveguide was first pumped out to its base pressure by turning off the flow controllers and opening the butterfly valve. A background mass spectrum was recorded at this base pressure. The flow of bottled air was then turned back on and the waveguide was flushed out for a short period. The waveguide was then sealed and filled to the desired pressure. A reference mass spectrum was recorded at this pressure to compare with later spectra.

The microwave pulse train was turned on at low power and the power was gradually increased until breakdown occurred in the waveguide. The power was then quickly reduced to just above breakdown threshold for the remainder of the power-on part of the experiment. The condition of the discharge was monitored with a small video camera looking through the viewing window into the waveguide, and also by observing the reflected power from the waveguide. Without breakdown, the shape of the reflected

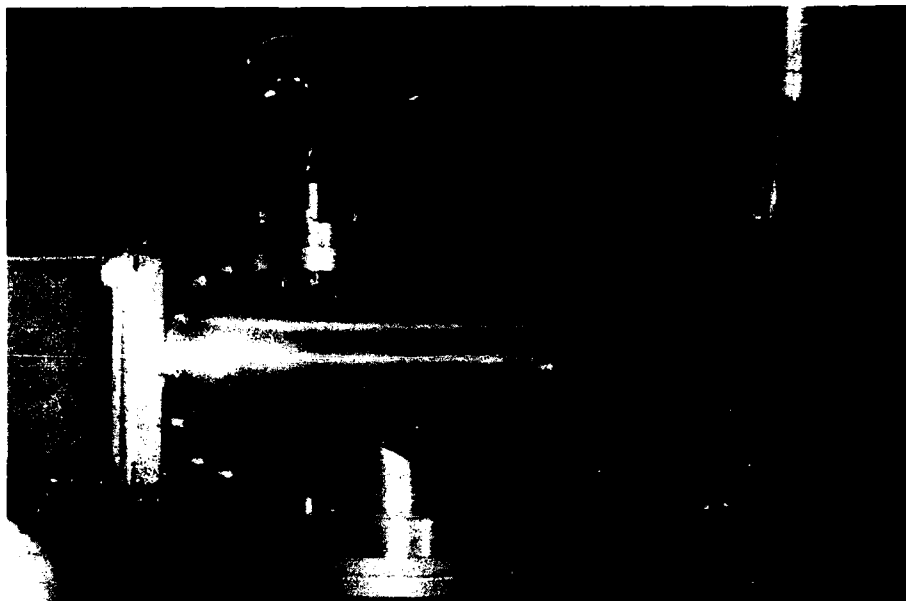


Figure 3. Photograph of Waveguide Test Section and Mass Spectrometer, Disassembled. The narrow waveguide test section is the vertical rectangular piece at the right and the mass spectrometer is the horizontal cylinder on the left. The sampling orifice into the mass spectrometer, the perforated screens in the waveguide, and the housing for the upper quartz window are visible.

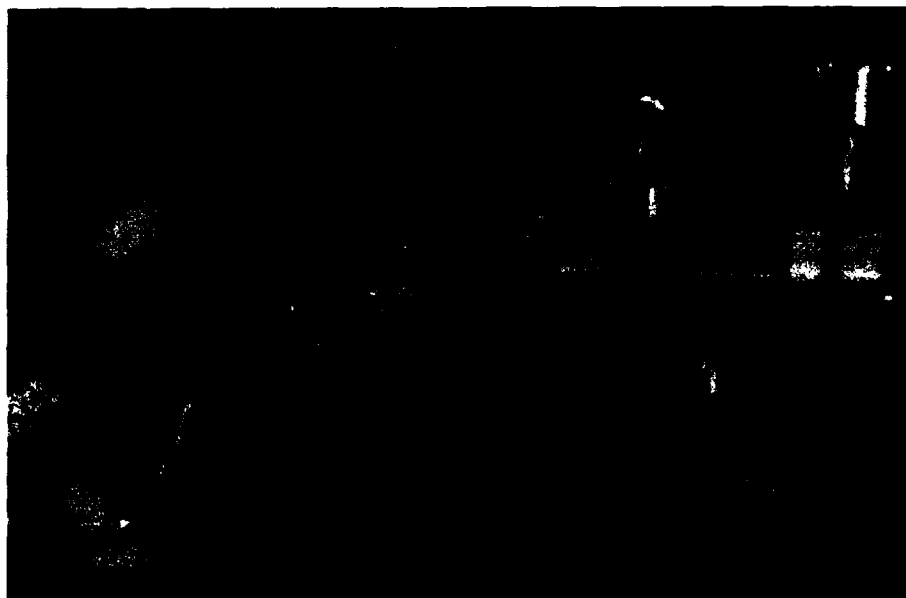


Figure 4. Photograph of Assembled Experiment. The clamping rings are now shown holding the mass spectrometer housing to the waveguide.

pulses was the same as the incident pulses. However, after breakdown occurred, the shape of the reflected pulse was changed considerably by interference effects caused by reflections from the plasma. The onset of breakdown within each pulse was clearly marked by a decrease in reflected power compared to the incident pulse. The incident power was adjusted in most experiments to the lowest level that gave reproducible, stable reflected power curves. This point was defined as the threshold. Typical incident and reflected pulses for low pressure in the waveguide are shown in Figure 5.

The microwaves were left on for 10 minutes, during which period a mass spectrum of the gas in the waveguide was recorded every one to two minutes. The microwaves were then turned off, and mass spectra continued to be recorded for another 10 minutes. A stopwatch was started when breakdown was first observed visually in either the video camera display or the reflected power pulse shape display. Timing accuracy is therefore within a few seconds. The mass spectrometer required about 10 seconds to record each mass spectrum. As will be seen later in this report, great accuracy in timing events was not needed because changes generally took place in a matter of minutes rather than seconds.

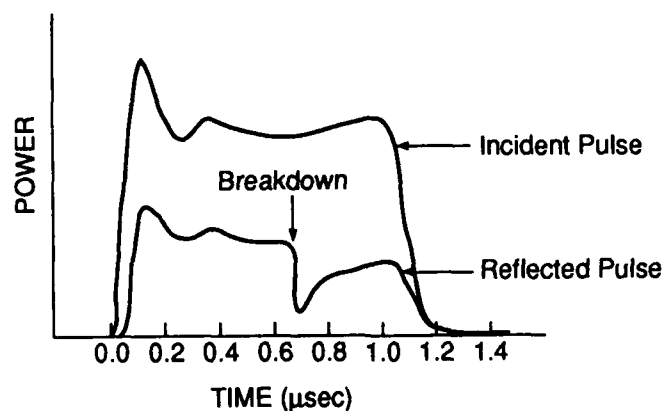


Figure 5. Typical Incident and Reflected Pulse Shapes. Breakdown occurred when the reflected power suddenly decreased.

4. CALIBRATION APPARATUS

After the plasma composition experiments at Livermore had shown that significant concentrations of nitrogen oxides were formed in the air breakdown regions, the mass spectrometer was returned to the Geophysics Laboratory to measure the sensitivity of the instrument to those gases. The calibrations were performed on a test stand similar to those that have been described in previous reports. The test stand is shown schematically in Figure 6.

The instrument was mounted to a small vacuum chamber pumped with an ion pump and a CTI Cryotorr 7 Cryopump. The base pressure in this chamber was 2×10^{-8} Torr. A test gas was introduced into the vacuum chamber through a variable leak valve, while the pressure in the chamber was monitored with Bayard-Alpert ionization gauges. In a typical calibration run, the ionization gauges were degassed at the start of the run, and then mass spectra were recorded at frequent pressure intervals between the base pressure and 1×10^{-4} Torr.

For the nitrogen oxide calibrations, test gas mixtures were prepared in a 1 liter metal gas bulb. A 0-1000 Torr capacitance manometer was directly attached to the bulb to measure the bulb pressure. This manometer was not affected by changes in gas composition, as some other pressure gauges are. After pumping out the bulb and flushing it with dry nitrogen, a small amount (0.5 - 10 Torr) of NO, NO₂ or N₂O was introduced into the bulb. The bulb was then filled with dry nitrogen to about 500-600 Torr. For each gas, test mixtures containing approximately 0.1, 1 and 2 percent of the gas were prepared.

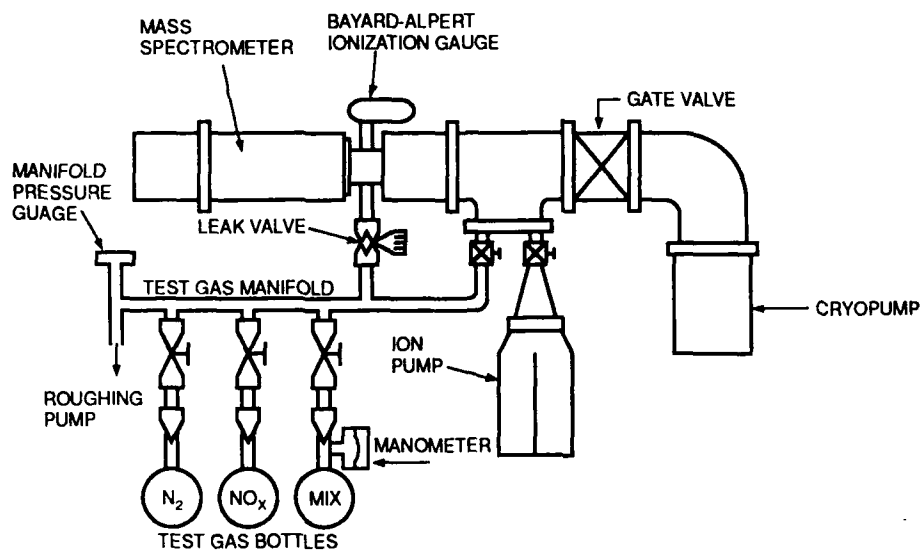


Figure 6. Calibration Test Stand at the Geophysics Laboratory

5. RESULTS

The changes in gas composition measured with the mass spectrometer caused by microwave breakdown varied dramatically with the pressure in the waveguide. From 25 to 200 Torr, nitric oxide, NO, was formed very quickly after the discharge was turned on. The time resolution of the experiment was not sufficient to measure the rise time of NO. However, we noted that by 15 seconds after breakdown, the shortest time difference we could measure, the NO concentration had reached its equilibrium value. It stayed at approximately this same value for as long as the breakdown was on. After the microwaves were turned off, the NO concentration decreased slightly. At the same time, the concentration of nitrogen dioxide, NO₂, rose from below the detection limit to slightly less than the NO concentration. The absolute concentrations of NO and NO₂ varied with pressure throughout the high pressure range, but their qualitative behavior was the same.

At lower pressure, 0.3 to 9 Torr, neither NO nor NO₂ were observed. Rather, the concentration of nitrous oxide, N₂O, increased as soon as the breakdown was turned on, and remained high after the breakdown was

turned off. Again, the concentration of N_2O varied with pressure in the waveguide, but qualitatively the behavior was the same at all pressures in the lower range.

Representative raw mass spectra for these two different regimes are shown in Figures 7 (200 Torr) and 8 (1 Torr). In each figure, the top panel shows a reference mass spectrum taken before the discharge was started. These are normal air spectra. The peaks are identified in Table 1. The resolution used for these spectra was quite high to separate 28, 29, and 30 and also 44 and 46 definitively. Consequently, there is some mass discrimination, and the low mass peaks are quite narrow and not as high as they should be.

The middle panel in Figure 7 shows a spectrum taken when the discharge was turned on at 200 Torr. As described above, the NO peak at mass 30 has increased dramatically compared with the reference spectrum. The bottom panel then shows a spectrum taken after the discharge was turned off. The NO peak remains high, and the NO_2 peak at mass 46 has increased significantly.

Table 1: Peak Identifications in Air Spectra

Mass	Identification
14	N^+ from dissociative ionization of N_2
16	O^+ from dissociative ionization of O_2
18	Water parent peak
20	Ar^{++}
28	Nitrogen parent peak
29	$^{14}\text{N}^{15}\text{N}$ nitrogen isotope peak
30	Nitric Oxide, NO, formed in ion source
32	Oxygen parent peak
34	$^{16}\text{O}^{18}\text{O}$ oxygen isotope peak
40	Argon parent peak
44	Carbon dioxide parent peak

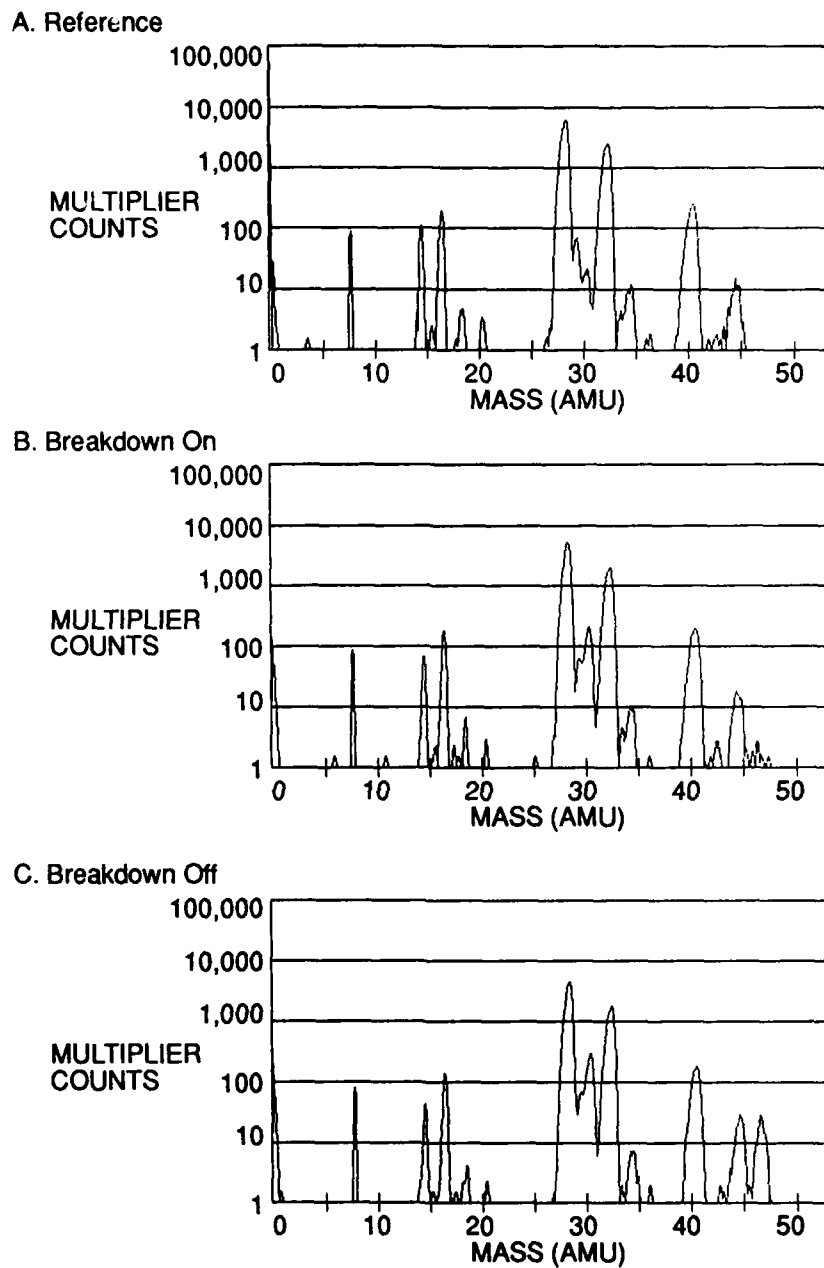
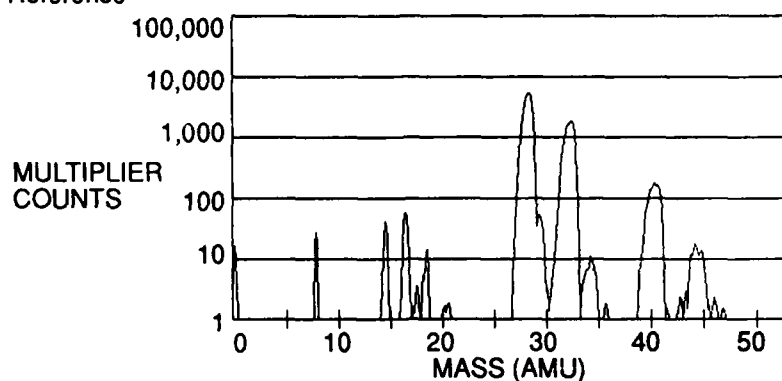


Figure 7. Representative Mass Spectra, 200 Torr. These three mass spectra are typical of the high pressure regime (25-200 Torr). Panel A shows a normal, background air spectrum, panel B shows the appearance of NO (mass 30) when the discharge was turned on, and panel C shows the subsequent rise of NO₂ (mass 46) after the discharge was turned off.

A. Reference



B. Breakdown On

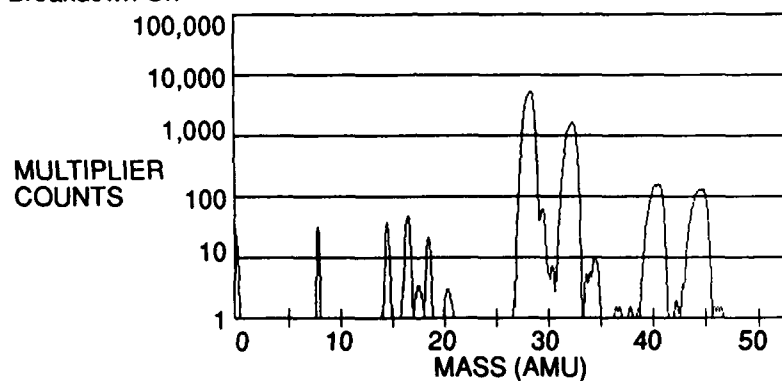


Figure 8. Representative Mass Spectra, 1 Torr. These two mass spectra are representative of the low pressure regime (0.3 - 10 Torr). Panel A again shows a normal, background mass spectrum, and panel B shows the change in nitrous oxide (N_2O) peak height at mass 44 after the discharge was turned on.

In Figure 8, the bottom panel shows a representative mass spectrum at 1 Torr taken after the discharge was turned on. The mass 44 peak has increased considerably. The small increase in mass 30 is consistent with dissociative ionization of N_2O in the ion source. There were no important differences in the spectra after the discharge was turned off compared with when it was on.

The heights of the mass 28, 32, 30, 44 and 46 peaks are plotted versus time in the next two figures. Figure 9 contains data from an experimental run at 100 Torr, where the phenomena observed were typical of the high pressure cases. As described above, the NO peak at mass 30 rose quickly after breakdown occurred, the NO_2 peak at mass 46 rose only after the breakdown was turned off, and the N_2O peak at mass 44 was essentially unchanged throughout the experiment.

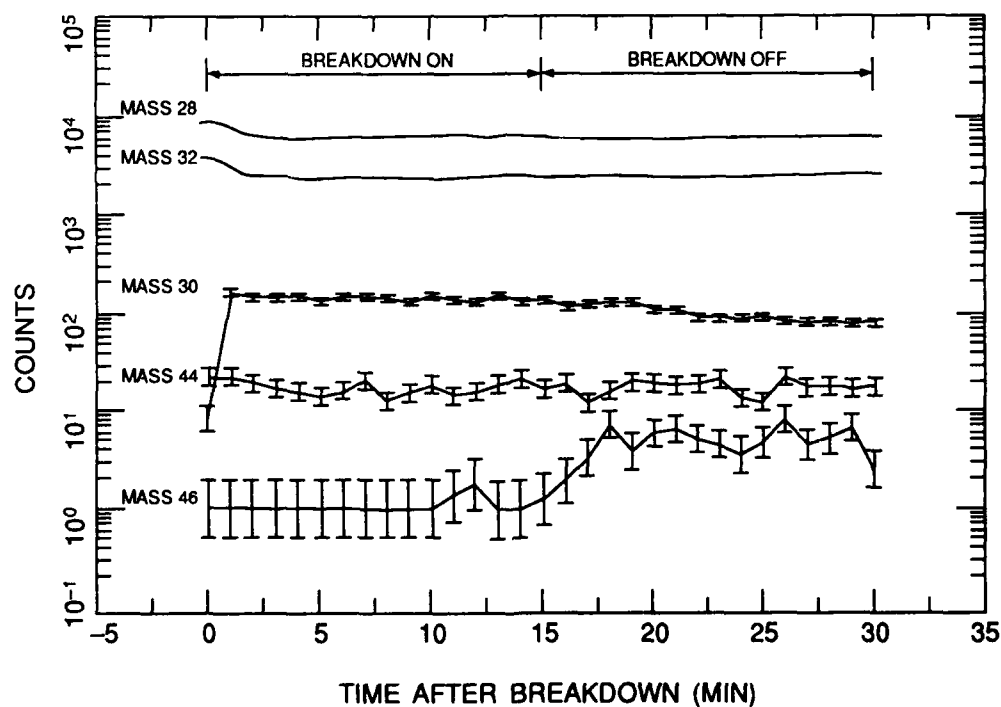


Figure 9. Time History of Peak Heights, 100 Torr. The heights of the mass 28, 30, 32, 44 and 46 peaks (measured in number of counts) are plotted against experiment time in minutes.

Figure 10 shows the time history of the same five mass peaks for an experimental run at 1 Torr. The N_2O peak at mass 44 rose noticeably after breakdown occurred, while the NO and NO_2 peaks were not greatly affected.

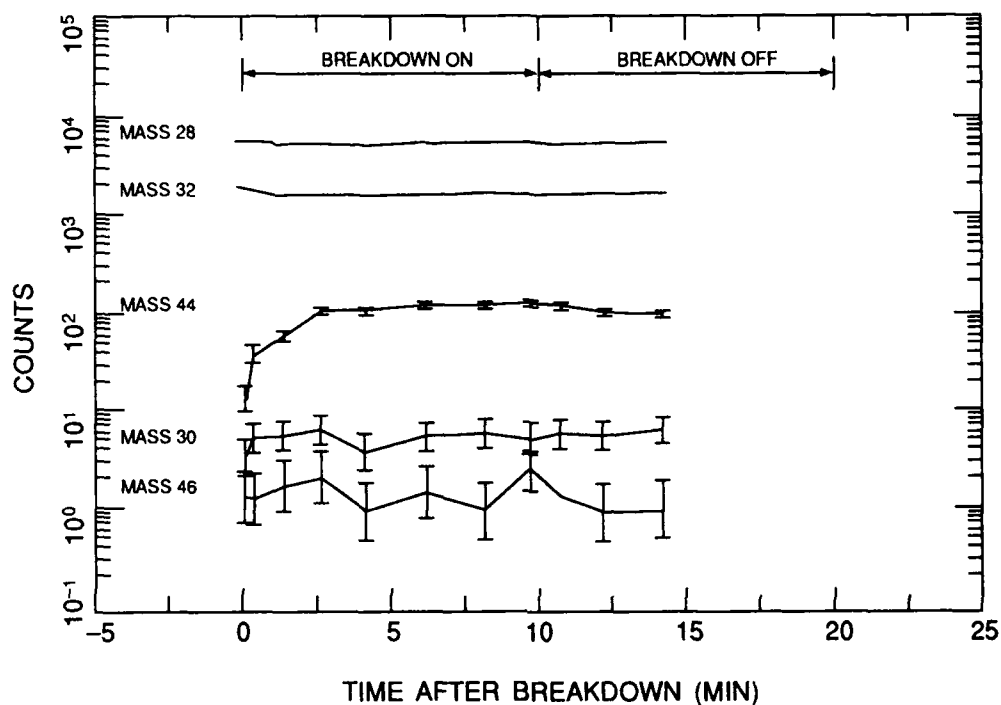


Figure 10. Time History of Peak Heights, 1 Torr

The slight decreases in the mass 28 and 32 peak heights seen in both Figures 9 and 10 are fairly consistent and reproducible. The data from Figure 9 are replotted in Figure 11 to emphasize the changes. The N_2 and O_2 signals have been normalized to their $T=0$ value before the microwaves were turned on. The normalized grid current measurements are also plotted in the Figure. As discussed in the experimental section of this report, the grid current is the total positive ion current collected on a 90 percent transmitting grid in the ion source of the mass spectrometer. This current can be related to the total pressure in the ion source, and is therefore an independent measure of the total amount of ion signal reaching the mass filter.

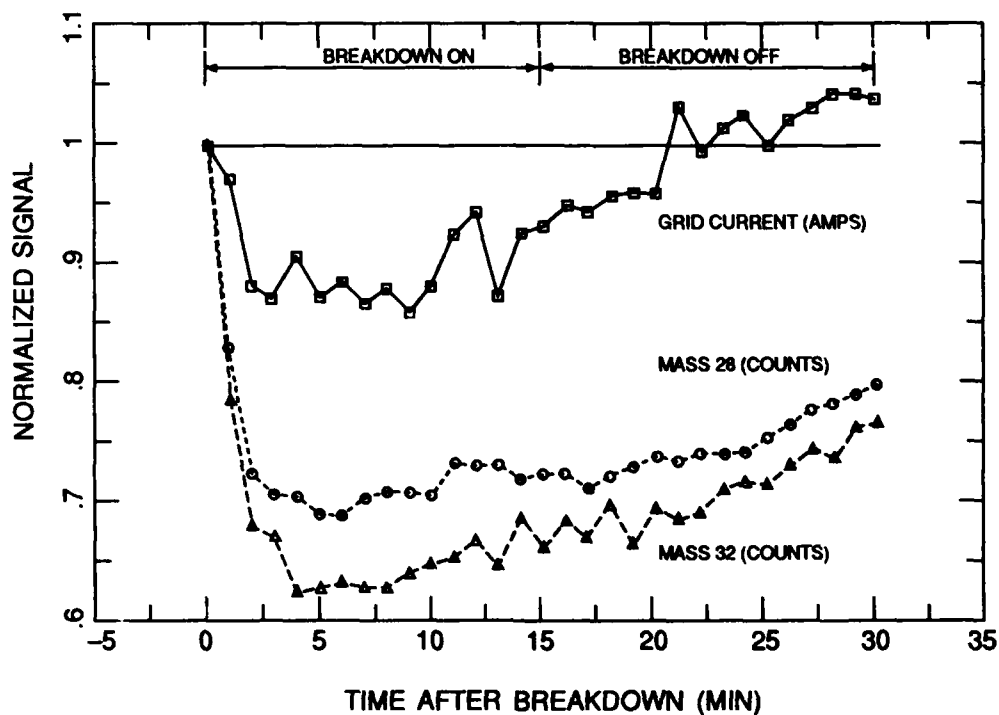
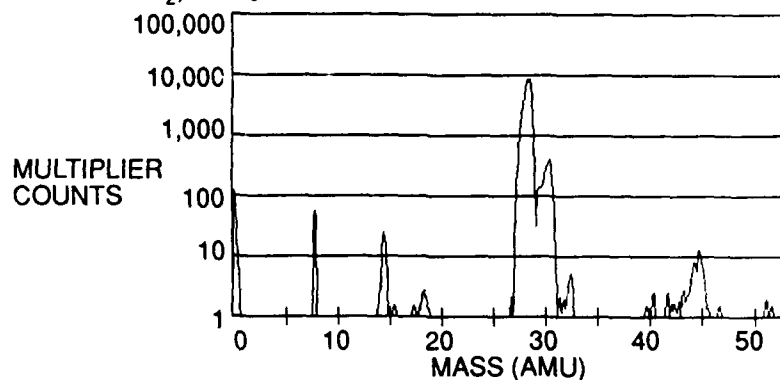


Figure 11. Detailed Time Histories of Mass 28, 32, and Grid Current. The data from Figure 9 are replotted to emphasize changes in the largest parent peaks. Each type of data has been normalized to its own T=0 value.

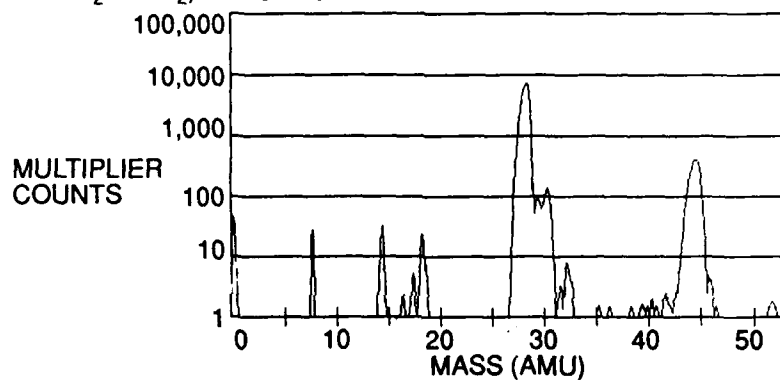
It is intriguing that the grid current and the two mass peaks behaved so differently. The grid current dropped by a little more than 10 percent during the discharge-on period and then rose to slightly higher than its pre-discharge level. The nitrogen and oxygen peaks, on the other hand, dropped by 30-40 percent and did not regain their T=0 levels in the time of the experiment. The changes in peak heights and the differences between the grid and the mass filtered data may be due to a combination of local heating and then overall heating of the gas in the waveguide, dissociation of the oxygen and nitrogen, and diffusion within the waveguide.

Typical calibration mass spectra taken at the Geophysics Laboratory after the Livermore experiment are shown in Figure 12. The three spectra

A. 2.0% NO in N₂, 3×10^{-5} Torr



B. 2.4% N₂O in N₂, 1×10^{-5} Torr



C. 2.1% NO₂ in N₂, 3×10^{-5} Torr

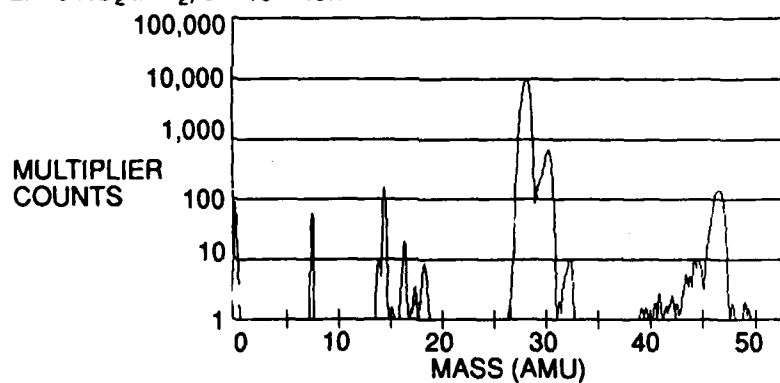


Figure 12. NO, NO₂ and N₂O Calibration Spectra. In each case, the gas mixture was approximately 2 percent NO_x in N₂, and the operating pressure in the ion source was 1×10^{-5} torr.

are of 2 percent mixtures of the NO_x species in nitrogen with an operating pressure in the mass spectrometer of 1×10^{-5} Torr. They demonstrate the different sensitivity of the mass spectrometer to the three gases and also show the "cracking patterns" of the molecules in the ion sources, that is, the pattern of ion signals at masses different from the parent ion signals.

The calibration data were used to calculate the relative sensitivity of the instrument to the NO_x species of interest compared with nitrogen. Comparisons were made to both the mass 28 primary peak of nitrogen and the mass 29 isotope peak. When the mass 28 signals were too high and neared saturation, the sensitivity comparison was made to the mass 29 isotope peak.

The calibration experiment results were used to convert the number of counts shown in the previous figures to actual pressures of the trace NO_x species. Because the mass spectrometer was differentially pumped, the pressure in the instrument's ion source was many orders of magnitude less than the waveguide pressure. Therefore, the mass spectrometer data could not be used to measure the partial pressures of the trace gases directly. Instead, the mass spectra were used to measure the relative concentrations of NO_x compared to nitrogen, and then were converted to absolute concentrations by using the waveguide pressure measured by the capacitance manometers. In calculating the partial pressures, the raw counts at each mass were corrected for dissociative ionization of higher mass species that contributed some signal. (For example, both NO_2 at mass 46 and N_2O at mass 44 produce some signal at mass 30. These signals must be subtracted before the NO concentration is calculated from the mass 30 counts.) The differences in relative sensitivity were also accounted for.

One example of converting raw counts to partial pressures is shown in Figure 13. The mass 46 counts taken from one of the 200 Torr runs have been converted to NO_2 partial pressures. The qualitative behavior, of course, is the same as shown in Figure 9, where the mass 46 counts stay at the detection limit until the discharge is turned off, and then rise to a final value. The detection limit for each gas at each waveguide pressure was taken to be that partial pressure at which two counts of signal would be detected.

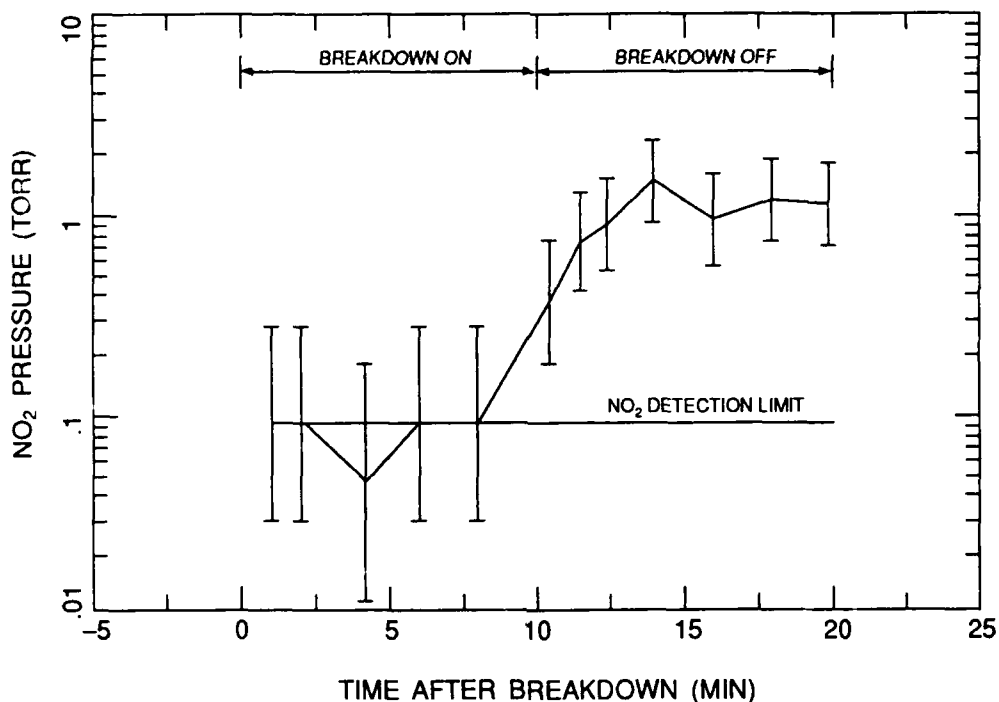


Figure 13. NO₂ Partial Pressure vs Time, 200 Torr

For each experimental run at each pressure, the final or asymptotic pressure for the three NO_x species was calculated in the same way. These results are summarized in Figures 14 - 16, where final NO, NO₂ and N₂O partial pressures, respectively, are plotted against the waveguide pressure. The break in detection limit that occurs at a waveguide pressure of about 10 Torr is due to a change in orifice size. All high pressure data, from 25 to 200 Torr, was taken with a 0.001" diameter orifice, whereas the low pressure data, from 0.3 to 9 Torr, was taken with a 0.005" diameter orifice.

Table 2 is a summary of the experimental conditions used for all of the experiments reported in Figures 14 - 16, and Table 3 is a list of the results.

Table 2: Summary of Experimental Conditions

Run No.	Pressure (Torr)	Flow (SL/m)	Power (kW)	Rep Rate (Hz)	Power On (Minutes)	Power Off (Minutes)	Orifice (Inches)
1	100	0	24	315	15	15	.001
2	100	0	25	314	10	10	.001
3	200	0	62	316	10	10	.001
4	200	0	53	316	6	10	.001
5	100	0	8.0	316.5	10	10	.001
6	100	0	11	315	10	9	.001
7	50	0	1.9	316.5	10	10	.001
8	50	0	8.3	316.8	10	10	.001
9	50	0	8.2	315	10	10	.001
10	25	0	2.8	316.9	10	10	.001
11	9	0.020	0.58	315	10	6	.005
12	9	0	0.85	315	10	10	.005
13	9	0	0.80	315	10	10	.005
14	5	0	0.46	315	10	10	.005
15	5	0	0.46	315	5	0	.005
16	1	0	0.16	315	10	4	.005
17	0.3	0	0.32	315	10	4	.005
18	1	0	0.13	315	10	10	.005
19	1	0	0.18	315	10	6	.005
20	1	0	0.26	315	10	6	.005
21	1	0	0.15	100	10	6	.005
22	1	0	0.21	33.3	10	6	.005

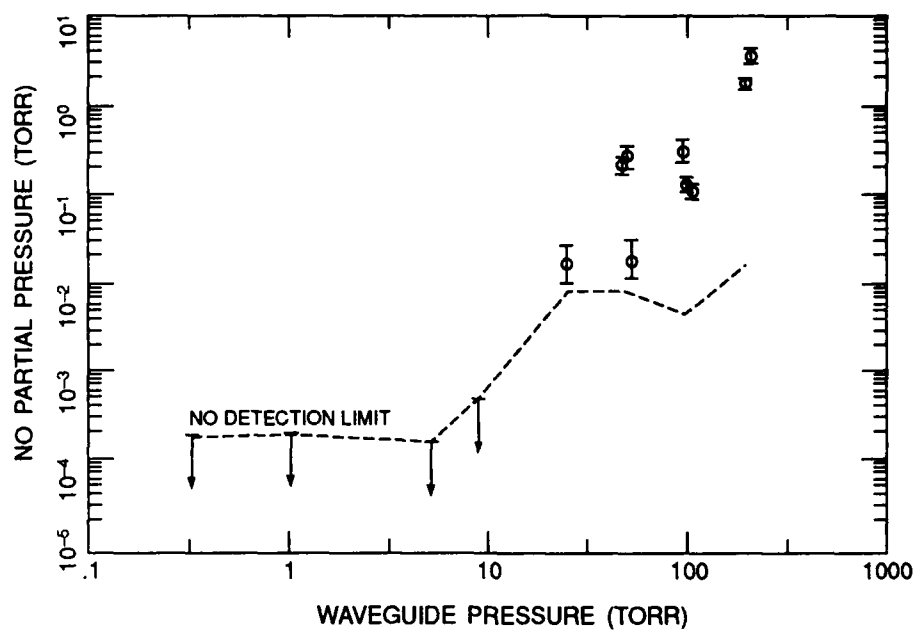


Figure 14. Asymptotic NO Partial Pressures

Notes on Figures 14, 15, and 16: For each experimental run at each waveguide pressure, the number of counts at masses 30, 44, and 46 at the end of the 10 minute microwave-off period were converted to NO_x partial pressures in the same way as for Figure 13. These asymptotic pressures are plotted against the air pressure in the waveguide. The detection limit in each case is the pressure that would give two counts of signal.

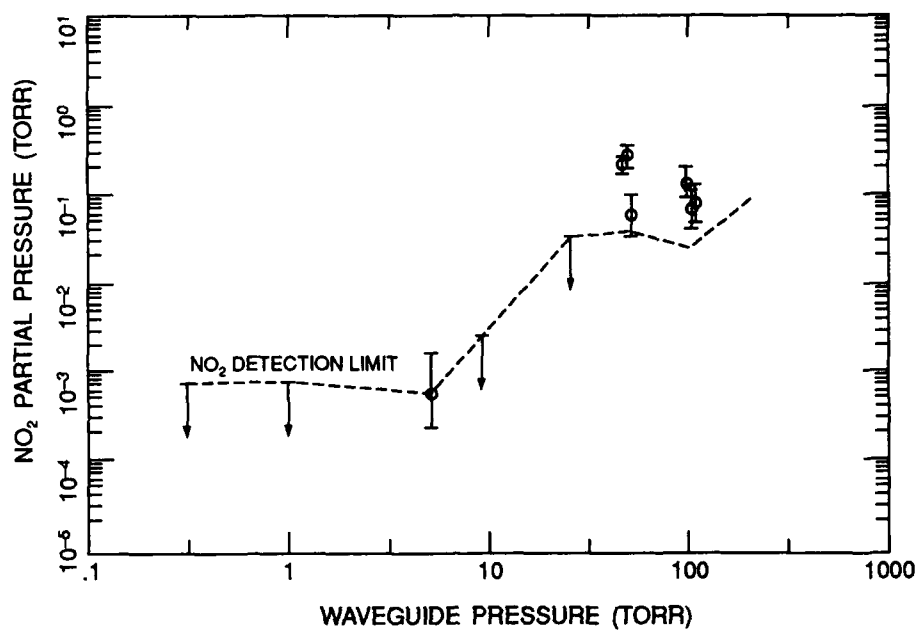


Figure 15. Asymptotic NO_2 Partial Pressures

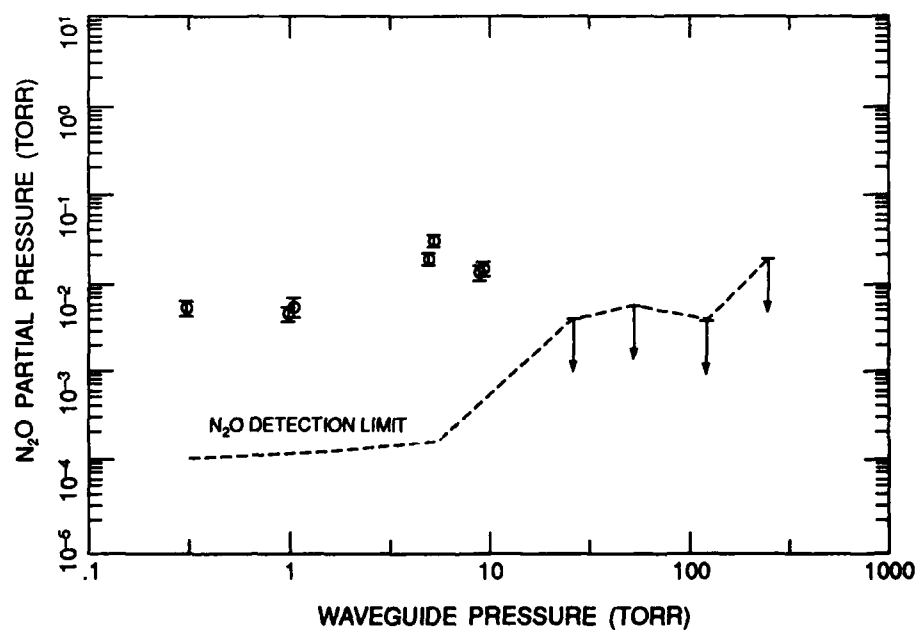


Figure 16. Asymptotic N_2O Partial Pressures

Table 3: Summary of NO, NO₂ and N₂O Asymptotic Partial Pressures

RUN #	PRESS. Torr	NO			N ₂ O			NO ₂		
		PRESSURE	ERROR	DET.LIMIT	PRESSURE	ERROR	DET.LIMIT	PRESSURE	ERROR	DET.LIMIT
3	200	3.72	.85	1.57E-2	.103	.019	1.68E-2	1.24	.38	8.95E-2
4	200	1.82	.25	1.75E-2	0	0	1.87E-2	.94	.35	.10
1	100	.109	2.4E-2	4.14E-3	0	0	4.42E-3	8.81E-2	4.9E-2	2.36E-2
2	100	.133	2.7E-2	3.85E-3	0	0	4.12E-3	7.32E-2	4.30E-2	2.19E-2
6	100	.314	.102	5.88E-3	0	0	6.29E-3	.149	7.68E-2	3.35E-2
7	50	1.80E-2	1.26E-2	6.71E-3	0	0	7.18E-3	0	0	3.82E-2
8	50	.26	.087	9.31E-3	0	0	9.96E-3	0	0	5.30E-2
9	50	.21	.045	7.34E-3	0	0	4.52E-3	6.21E-2	4.2E-2	3.10E-2
10	25	1.65E-2	1.1E-2	8.34E-3	0	0	5.14E-3	0	0	3.52E-2
12	9	0	0	3.54E-4	1.63E-2	2.7E-3	3.79E-4	0	0	2.06E-3
13	9	0	0	6.08E-4	1.45E-2	3.3E-3	6.5E-4	0	0	3.46E-3
14	5	0	0	2.21E-4	3.36E-2	4.8E-3	2.36E-4	0	0	1.26E-3
15	5	0	0	8.6E-5	2.09E-2	2.79E-3	8.28E-5	6.7E-4	1.13E-3	6.3E-4
16	1	0	0	2.03E-4	5.72E-3	1.78E-3	1.25E-4	0	0	8.60E-4
18	1	0	0	1.92E-4	4.77E-3	7.9E-4	1.18E-4	0	0	8.1E-4
17	0.3	0	0	1.89E-4	5.47E-3	9.7E-4	1.16E-4	0	0	8E-4

Table 4. Summary of Optical Absorbance Measurements

Waveguide Pressure (Torr)	Measurements of NO ₂ Pressure (Torr)
200	0.88, 0.54
100	0.11, 0.11, 0.12
50	0.0024, 0.21, 0.21
25	0.0018

Though the optical absorbance measurements taken simultaneously with the mass spectrometer measurements have not been discussed in any detail here, the results of that experiment are summarized in Table 4. The bandpass of the filter was chosen to coincide with an absorption feature of NO₂, and so the measurement was sensitive only to the NO₂ partial pressure in the waveguide. Comparing the NO₂ pressures in Table 4 with the mass spectrometric measurements in Table 3 and Figure 16 shows that the two measurement techniques are in agreement with each other to within a factor of 2.

The trends in these data can be seen more easily in Figure 17, where the mole fraction of each trace gas is plotted against waveguide pressure. The mole fraction is the partial pressure of the trace gas divided by the total waveguide pressure. At high pressures, NO is the most concentrated species, reaching a concentration of nearly 2 percent. NO₂ is somewhat less concentrated. Both of these gases decrease in fractional content as the pressure is reduced, reaching a minimum at about 25 Torr. Below that pressure, N₂O is the major species. It rises in relative concentration as the pressure decreases, reaching a maximum of about 2 percent at 0.3 Torr.

A further simplification of the data is shown in Figure 18. The total fractional content of NO_x species is the sum of the NO, NO₂ and N₂O partial pressures divided by the total pressure. This total fractional NO_x concentration is plotted against total pressure, and again shows that the

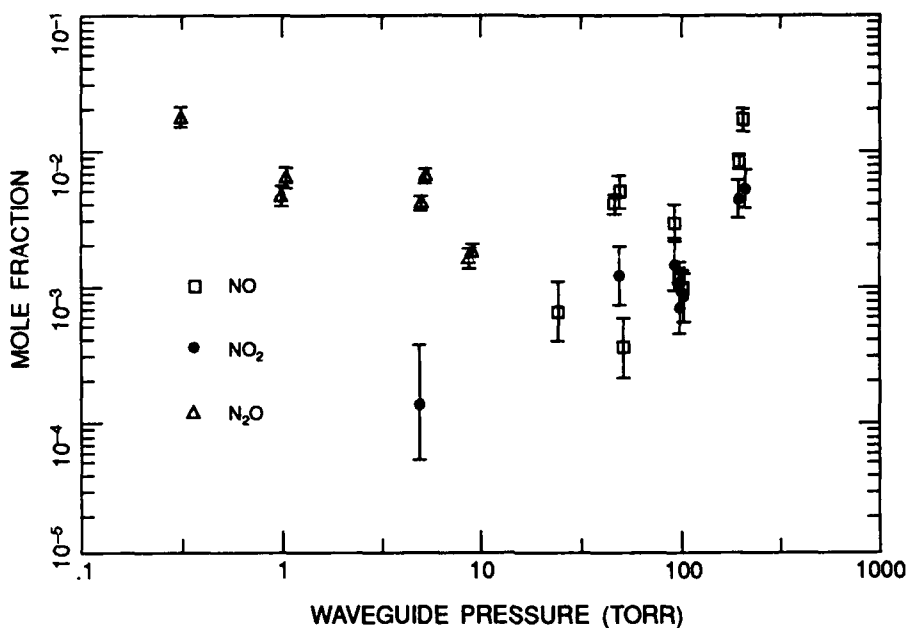


Figure 17. Mole Fractions of NO, NO₂ and N₂O vs Waveguide Pressure

highest concentrations are seen at the extreme pressures studied, while a minimum is seen in the middle at about 25 Torr.

Finally, two other experiments were done with a total pressure of 1 Torr in the waveguide to examine the effect of microwave pulse power and pulse repetition rate on the N₂O concentration. In the first experiment, the effect of the power was monitored by observing the reflected power in the same way as described above for setting the breakdown threshold. The conditions were 50.6 dBm at threshold for formation of a single breakdown region, 52.4 dBm for formation of a second breakdown region and 54.3 dBm for formation of the third region. The repetition rate was 315 Hz in each case. The N₂O concentration formed in each case is plotted in Figure 19 against the microwave pulse power, and shows a clear increase of a factor of around 3.5 with the increase in power.

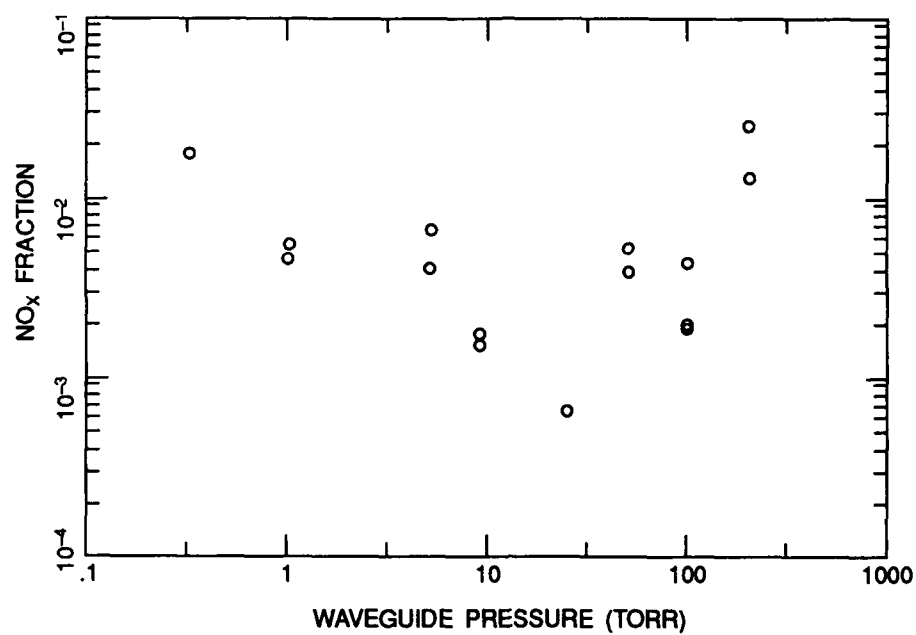


Figure 18. Total Fractional Content of Nitrogen Oxide Species vs Waveguide Pressure

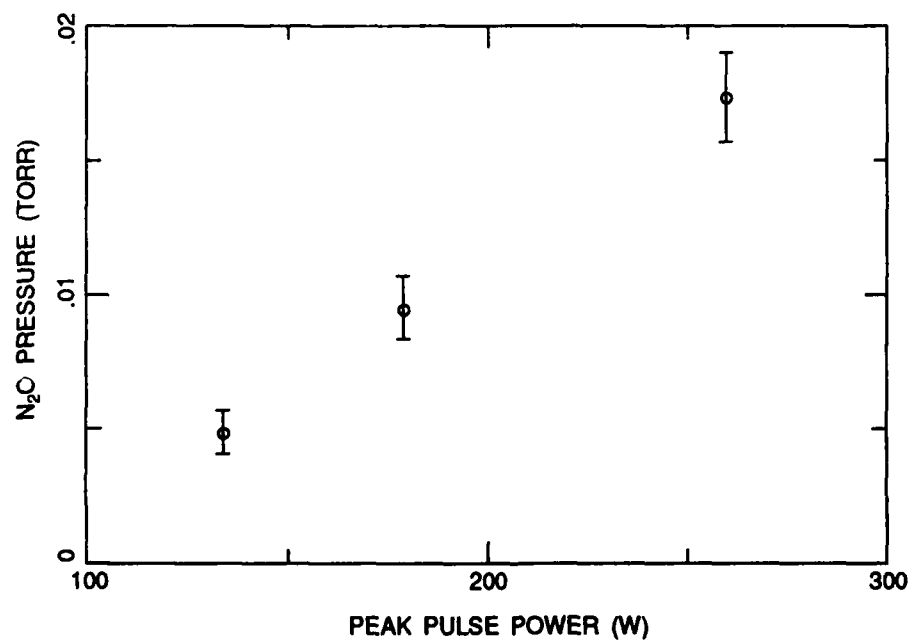


Figure 19. Microwave Power Dependence of N₂O Concentration at 1 Torr

In the second experiment, the repetition rate of the pulse train was reduced from 315 Hz to 100 Hz and then to 33 Hz. In each case, the power was set just above breakdown threshold. Because the interpulse period increased, however, the amount of residual ionization decreased at the end of the interpulse period, and the pulse power had to be increased slightly to cause breakdown at the lower repetition rates. Figure 20 shows a slight decrease in N_2O concentration with decreased repetition rate, a decrease that would be more dramatic if the data were corrected for changes in power.

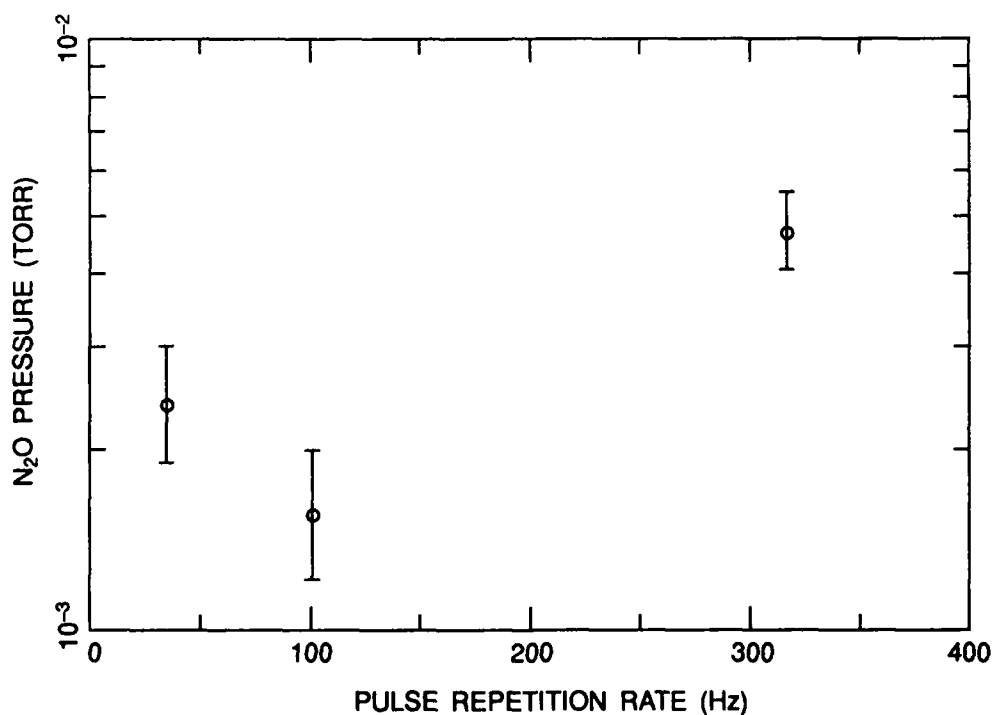


Figure 20. Dependence of N_2O Concentration on Pulse Repetition Rate at 1 Torr

6. DISCUSSION

To assess the validity of the data reported here, we have examined a number of possible sources of anomalies. These are the potential effects of ultraviolet light, the ion-molecule reactions that can occur in the ion source, and the possible effects of changing the orifice size. We tentatively conclude that none of these had an important effect on the data.

Ultraviolet light emitted from excited species in the plasma can, in principle, cause a number of problems in mass spectrometric measurements: photoelectrons emitted from metallic surfaces near the electron multiplier detector in the mass spectrometer can lead to spurious background counts, and photoionization of neutral species in the ion source of the instrument can lead to increased ion signals. Neither of these potential problems seems to affect the present measurements, however. The mass spectra plotted in Figures 7 and 8 have not had any background subtracted from them; they are unaltered raw spectra. The background level in all of them is at zero counts whether the plasma is on or off, showing that photoelectrons do not change the background level. Also, there are no sudden drops in any of the signals when the plasma is turned off, which indicates that photoionization is not an important source of ion signal.

Neutral and ion reactions can occur in the ion source of a mass spectrometer and alter the apparent composition of the gas being measured. For example, the small amount of mass 30 signal, due to NO, in the top panel of Figure 7 is formed this way: some neutral NO is manufactured in mass spectrometer ion sources. It is possible that the NO_x species apparently formed by the plasma discharge might be due to reactions occurring in the ion source between, perhaps, excited N₂ and O₂ species that do not occur with cold air. The data are not consistent with this idea, however. After the microwaves are turned off, the concentrations of nitrogen oxide species reach equilibrium values after several minutes, and do not change appreciably after that. If these molecules were being produced solely by excited state reactions between other N- and O-containing species in the ion source, we would expect that the amounts of those excited states would decline steadily with time as they are quenched by gas phase collisions. The

measured amounts of nitrogen oxides would then decrease steadily, also. The data are more consistent with formation of stable neutral species that fill the waveguide and are sampled as the gas flows through the orifice into the mass spectrometer. Further investigation of this possible effect needs to account for the lifetimes of excited states that might be formed in the plasma.

All of the experiment runs that showed the presence of NO and NO₂ were done with the 0.001" orifice, whereas all the runs which showed N₂O were done with the 0.005" orifice. Unfortunately, an intermediate size orifice was not available to check the transition between these two regimes. It is obviously important to investigate whether the change in orifice size caused the change in observed gas composition.

A larger orifice could allow more ultraviolet light to enter the instrument. However, as discussed above, there does not seem to be any noticeable effect of UV light.

Further, the flow characteristics of the gas through the two orifices were similar. The pressures measured in the differentially-pumped mass spectrometer chamber were in the same range for the two different orifices. Since the pumping speed of the turbopump on this chamber was not changed by the orifice size, this shows that the volume of gas flowing through the orifice was in the same range for both orifices. Also, except for the lowest pressure for the larger orifice, the mean free path of the gas was smaller than the orifice diameter. The flow was therefore hydrodynamic, and the transition region to free molecular flow was not reached for either orifice.

One other potentially important difference between the two orifices has to do with the relative amount of surface with which the gas can interact. The thickness of the orifice plate was 0.005". Therefore, the smaller, 0.001" diameter, orifice was really a tube five times longer than wide. The gas passing through this small orifice had a better chance to interact with the metal surface than the gas passing through the larger orifice. The effect of surface interactions might be to change the internal state distribution of some gas molecules, and therefore change their behavior in the ion source. However, as discussed above, the behavior of the data is not consistent with excited state reactions in the ion source.

The best support for the mass spectrometer measurements comes from the optical absorption measurements of NO_2 concentration. Comparison of Table 4 with Figure 15 shows that the two types of measurements are in excellent agreement. At 200 Torr, the optical absorption measurements are slightly lower than the mass spectrometer measurement (by less than a factor of 2) and at 100 Torr, the two measurements are nearly identical. At 50 Torr, the agreement is less good. However, the mass spectrometer measurement was just a few counts above background, and so was not very accurate.

The slight differences between the two measurements may be due to the fact that the mass spectrometer measured a local concentration of gases at the position of the discharge, whereas the optical absorption technique measured an integrated concentration along the whole path length. However, both measurements show the trace gas concentrations reaching an asymptotic limit by the end of the experiment time. This probably means that the turbulence in the waveguide caused by the breakdown mixed the gases throughout the waveguide and that both measurements are of final, equilibrium concentrations.

7. SUMMARY

The changes in the composition of air inside a waveguide following breakdown induced by high power microwave pulses have been measured by mass spectroscopy and optical absorbance. The conditions for the experiment were as follows: Waveguide pressure: 0.3 - 200 Torr; Test gas in waveguide: bottled air; Microwave frequency: 2.856 GHz; Microwave pulse length: 1 microsecond; Microwave pulse repetition rate: 315 Hz; Microwave power: at breakdown threshold, which varied as a function of pressure.

The results from the two techniques are in excellent agreement. Below a pressure of 10 Torr in the waveguide, the main trace gas produced is nitrous oxide (N_2O). Between 0.3 Torr and 10 Torr, the amount of N_2O increases with *decreasing* waveguide pressure, reaching a maximum relative concentration of 2 percent. Between 25 and 200 Torr in the waveguide,

nitric oxide (NO) and nitrogen dioxide (NO₂) are observed, though the NO₂ does not appear until the microwave pulse train has been turned off. In this higher pressure range, the relative amount of NO and NO₂ increases with *increasing* pressure, again reaching a maximum concentration of 2 percent.

It is clear from this preliminary presentation of the data that the chemistry of air breakdown changes dramatically with air pressure. This suggests that the initial energy distribution of the electrons produced by the discharge, the production of excited states of atomic, molecular and ionic oxygen and nitrogen by electron impact, the subsequent reactions of those species, and the collisional quenching of the excited species and ions - all of which depend on the gas pressure - need to be accounted for in understanding the chemistry. Future reports will examine such effects, and will attempt to synthesize a complete picture of the air breakdown chemistry required to understand the data presented here.

References

1. Rusanov, V. D., Fridman, A. A. and Sholin, G. V. (1981) The Physics of a Chemically Active Plasma With Non-equilibrium Vibrational Excitation of Molecules, *Sov. Phys.-USP. (USA)*, **24** (No. 6): 447-74.
2. Zipf, E. C. (1980) A Laboratory Study on the Formation of Nitrous Oxide by the Reaction $N_2(A) + O_2 = N_2O + O$, *Nature*, **287**: 523-524.
3. Park, C. (1989) A Review of Reaction Rates in High Temperature Air, *AIAA-89-1740, AIAA 24th Thermophysics Conference*, Buffalo, New York, June 12-14, 1989.
4. Fraser, M. E., Tucker, T. R., Piper, L. G., and Rawlins, W. T. (1989) N_2O Production Mechanism From the Interaction of Discharge-Excited Species, Pre-publication manuscript.
5. Zinn, J., Sutherland, C. D., and Roussel-Dupre, R. (1989) Chemistry Calculations Relating to AIL, *Workshop on Artificial Ionized Layers in the Atmosphere*, Kiev, USSR, 9-13 October.
6. Hunton, D.E, Trzcinski, E., Wlodyka, L., Federico, G. and Dorian, J. (1986) Quadrupole Ion/Neutral Mass Spectrometer for Space Shuttle Applications, *AFGL Technical Report AFGL-TR-86-0084* ADA172000.